arXiv:cond-mat/0508023v1 [cond-mat.mes-hall] 31 Jul 2005

Exchange and correlation effects on drag in low density electron bilayers: Coulomb and virtual-optical-phonon-mediated electron-electron interaction

S. M. Badalyan [a,*], C. S. Kim [a], and G. Vignale [b]

[a] *Department of Physics and Institute for Condensed Matter Theory, Chonnam National University, Gwangju 500-757, Korea*

[b] *Department of Physics and Astronomy, University of Missouri - Columbia, Missouri 65211, USA*

Abstract

We investigate the effect of exchange and correlation (xc) in low-density electron bilayers. Along with the direct Coulomb interaction, the effective electron-electron interaction mediated by the exchange of virtual polar optical (PO) phonons is considered. We find that the introduction of xc corrections results in a significant enhancement of the transresistivity and qualitative changes in its temperature dependence. The virtual PO-phonon contribution behaves similarly to the Coulomb drag and reduces noticeably the total drag thereby resulting in a better agreement with the recent experimental findings.

Key words: exchange and correlations, drag, phonon, bilayers
PACS: 71.45.Gm, 73.20.Mf, 73.63.Hs

1. Introduction

Recently the drag measurements have been extended to the limit of very low carrier density. The dimensionless parameter $r_s = \sqrt{2}/(k_F a_B^*)$, which is used to describe the carrier density, n, and measures the strength of the electron-electron (e-e) interaction [1], varies approximately from 10 to 20 in the experiment on hole samples [2]. Here $k_F = \sqrt{2\pi n}$ is the Fermi wave vector, a_B^* the effective Bohr radius. In electron samples r_s is appreciably smaller [3], owing to the small electron mass. However, it is clear from the dimensional analysis that in both types of low-density samples, the Coulomb potential energy dominates the kinetic energy, and an adequate description of the drag cannot be provided by simple Boltzmann-equation theories [4], which do not include the strong exchange-correlation (xc) effects.

The interaction effects on drag have been addressed previously in several experimental [5,6] and theoretical [7,8] papers. While the theoretical prediction [7] of an enhancement of drag by plasmons has been experimentally verified [5] in high density electron samples, important differences have been reported [6] from the results obtained within the random phase approximation (RPA). Lately, motivated by the recent experiments [2,3], the transresistivity has been calculated in Refs. [9] and [10]. Both works have included only the exchange effects in the static limit via q-dependent but ω-independent local field factors (LFF). Besides, in

* Corresponding author. Also at: Department of Radiophysics, Yerevan State University, 1 A. Manoogian st., 375025 Yerevan, Armenia. Phone: 8262-530-0063, Fax: 8262-530-3369, Email address: badalyan@boltzmann.chonam.ac.kr

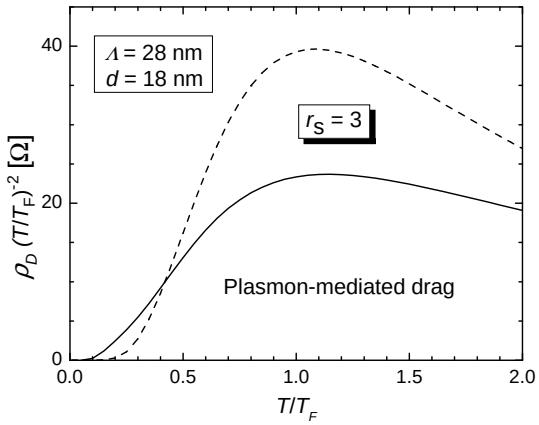

Fig. 1. Dynamic xc corrections to the plasmon-mediated drag for $r_s = 3$. The scaled transresistivity vs temperature is shown within the RPA (dashed curve) and beyond it including the intra- and inter-layer xc effects (solid curve).

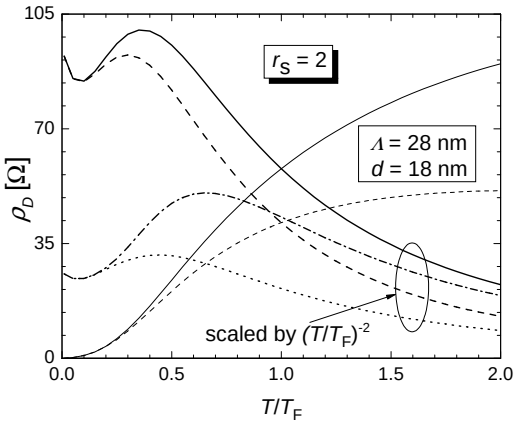

Fig. 2. The drag transresistivity vs temperature for $r_s = 2$. The solid and dashed (dash-dotted and dotted) curves represent the total ρ_D and the particle-hole contribution to ρ_D with the xc corrections included (within the RPA).

the adopted approximation the nondiagonal inter-layer LFF have been taken to be zero while for the intra-layer LFF the simple Hubbard approximation has been used, which significantly underestimates the LFF.

We propose a new approach making use of the dynamic xc kernels to study the xc effects on the drag in electron bilayers. The introduction of xc results in a significant enhancement of the drag rate and qualitative changes in its temperature dependence. In particular, a large high-temperature plasmon peak that is present in the RPA disappears when the xc corrections are included. We combine the direct Coulomb interaction with an effective e-e interaction, mediated by the exchange of virtual polar optical (PO) phonons. This new contribution to the drag improves noticeably a reasonably good agreement of our numerical results with the experimental findings by Kellogg *et al.* [3].

2. Theoretical formulation

The drag transresistivity is given by [11]

$$\rho_D = \frac{\hbar^2}{2e^2 n_1 n_2 T A} \sum_{\vec{q}} q^2 \int_0^\infty \frac{d\omega}{2\pi} |W_{12}(q,\omega)|^2 \times \frac{\mathrm{Im}\Pi_1^0(q,\omega)\mathrm{Im}\Pi_2^0(q,\omega)}{\sinh^2(\hbar\omega/2T)} \quad (1)$$

where A is the normalization area, $\Pi_{1,2}^0(q,\omega)$ the finite temperature electron polarization function of individual layers in the absence of inter-particle interaction. The xc effects on the dynamically screened inter-layer e-e interaction is approximated by $W_{12}(q,\omega) = V_{xc,12}(q,\omega)/\varepsilon_{bi}(q,\omega)$ with $\varepsilon_{bi}(q,\omega) = \varepsilon_1(q,\omega)\varepsilon_2(q,\omega) - V_{xc,12}(q,\omega)^2\Pi_1^0(q,\omega)\Pi_2^0(q,\omega)$ being the bilayer screening function [8,12]. Here we introduce the screening functions $\varepsilon_{1,2}(q,\omega)$ of individual layers. The intra- and inter-layer unscreened effective Coulomb interactions are given by

$$V_{xc,ij}^C(q,\omega) = v(q)\left(1 - G_{xc,ij}(q,\omega)\right) F_{ij}(qd, q\Lambda) \quad (2)$$

where the intra- and inter-layer LFF, $G_{xc,ij}(q,\omega)$, decrease effectively the bare Coulomb interaction, $v(q)$, by a factor of $1 - G_{xc,ij}(q,\omega)$. The form factors $F_{ij}(qd, q\Lambda) = \int dz dz' \rho_i(z)\rho_j(z') \exp(-q\,|z - z'|)$ are obtained making use $\rho(z) = (2/d)\,\sin(\pi z/d)^2$ for the electron density profiles. Here Λ is the inter-layer spacing and d the width of quantum wells.

The phonon-mediated effective unscreened e-e interaction, $V_{xc,ij}^{ph}(q,\omega)$, appears in second order perturbation theory with respect to the bare electron-phonon (e-p) coupling. Neglecting the weak energy dispersion of PO-phonons, we find that $V_{xc,ij}^{ph}(q,\omega)$ is proportional to the PO-phonon propagator $D_{PO}(\omega) = 2\hbar^{-1}\omega_{PO}/\left(\omega^2 - \omega_{PO}^2\right)$ and is represented as

$$V_{xc,ij}^{ph}(q,\omega) = \left(\frac{\kappa_0}{\kappa_\infty} - 1\right) \frac{\hbar\omega_{PO}}{2} D_{PO}(\omega) V_{xc,ij}^C(q,\omega) \quad (3)$$

where κ_0 and κ_∞ are the static and high frequency dielectric constants. We are interested in experimental

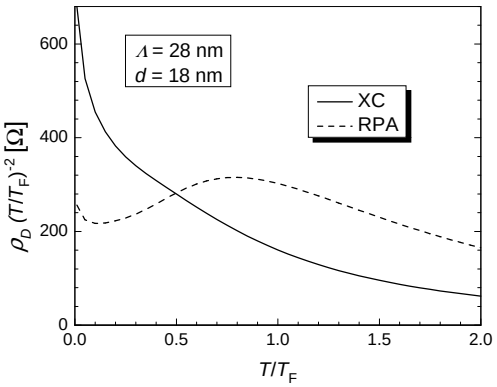

Fig. 3. The full xc corrections to the drag for $r_s = 3$. The dashed and solid curves represent the scaled transresistivity vs temperature, calculated, respectively, within and beyond the RPA. The RPA data are multiplied by a factor of 3.

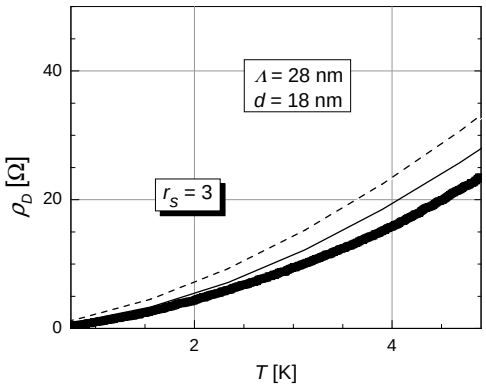

Fig. 4. The xc effect on the total drag (solid curve) for $r_s = 3$ due to the combined effect of direct Coulomb (dashed curve) and effective virtual-PO-phonon-mediated e-e interaction. The symbols are the experimental findings from Ref. [3] for $n = 3.8 \cdot 10^{10}$ cm^{-2}.

situations where T is much lower than the PO-phonon energy, $\hbar\omega_{PO} \approx 421$ K. Due to the energy and momentum conservation, the real PO-phonon emission and absorption processes are accompanied with a large energy and momentum transfer. Therefore, the resulting drag is negligibly small. This is clearly seen in Ref. [13] where the real-PO-phonon contribution to drag is obtained by a factor of e^{-28} smaller than the direct Coulomb drag. In stark contrast, scattering by virtual PO-phonons does not imply the energy and momentum conservation and provides an appreciable contribution to drag. Moreover, the main contribution to drag is made by scattering processes with the energy scale of $\omega \lesssim T \ll \omega_{PO}$ for which the PO-phonon propagator $D_{PO}(q,\omega)$ is far from the mass surface. Thus, the total unscreened e-e interaction, $V_{xc,ij}(q,\omega) = V^C_{xc,ij}(q,\omega) + V^{ph}_{xc,ij}(q,\omega)$, is well approximated by

$$V_{xc,ij}(q,\omega) = (2 - \kappa_0/\kappa_\infty)\, V^C_{xc,ij}(q,\omega). \qquad (4)$$

It is seen that the attractive e-e interaction, mediated by virtual PO-phonons, reduces the Coulomb interaction strength by a factor of $(2 - \kappa_0/\kappa_\infty)$. In GaAs taking $\kappa_0 = 13.18$ and $\kappa_\infty = 10.89$ [14], we have an about 21 percent reduction of the interaction strength. Notice that the reduction effect manifests itself also via the screening of interaction. The acoustical phonons, because of their weak e-p coupling and small energy with the strong linear dispersion, have no such universal effect on drag and are not considered here.

To obtain the bilayer LFF $G_{xc,ij}(q,\omega)$ we interpret the layer index as an isospin and represent the intra- and inter-layer LFF in terms of the "spin-channel" and "charge-channel" LFF. When treating the plasmon contribution to the drag, we employ the dynamic spin-spin and charge-charge xc kernels, evaluated by Qian and Vignale [15]. The frequency-dependence of the LFF in the particle-hole continuum region (finite wave vector, low frequency) is still largely unknown. For this reason, in evaluating the particle-hole contribution to the drag, we use the static limit of the LFF taking advantage of the analytical expressions recently obtained for the spin-spin and charge-charge LFF [16].

3. Many-body corrections to the total drag transresistivity

In Fig. 1 we show the effect of the intra- and inter-layer dynamic xc on the plasmon-mediated drag by comparing the obtained results with those of RPA-based calculations for the symmetric bilayer systems with $r_s = 3$. It is seen that the upturn temperature in the scaled transresistivity vs temperature essentially decreases when the xc effects are included. The plasmons begin to contribute heavily at temperatures about $0.1T_F$, which is approximately a factor of 2 smaller than the upturn temperature calculated within the RPA. The effect is slightly weak for $r_s = 2$. At the relatively high temperatures, the average energy of plasmons that mediate the drag increases. Hence, the plasmon damping, caused by dynamic xc effects, becomes stronger with a consequent reduction

in the drag transresistivity. Thus, around $0.4T_F$ the plasmon-mediated drag obtained within the RPA exceeds the drag which takes into account the full xc effects. Notice also that at even higher temperatures the differences in the magnitude of drag in the different approximations diminishes with increasing T.

In Fig. 2 we plot the drag transresistivity vs temperature within and beyond the RPA for $r_s = 2$. It is seen that in both approximations the particle-hole contribution to the scaled drag transresistivity first shows a slight dip followed by a peak at higher temperatures. In the RPA the plasmon contribution to drag enhances this peak and shifts it to even higher temperatures so that the total transresistivity shows a pronounced peak approximately at the position where the plasmon contribution has a peak. The introduction of the static exchange-controlled LFF increases the peak height of the particle-hole contribution to the drag and shifts the peak towards lower temperatures. On the other hand, the plasmon-mediated drag is moderately suppressed by the dynamic xc corrections (cf. Fig. 1). Thus, the resulting peak in the graph of the total transresistivity vs temperature remains a small feature at relatively low temperatures, while at high temperatures the drag rate shows a monotonic decrease in T.

The described quantitative and qualitative differences in the behavior of the scaled total transresistivity within and beyond the RPA becomes more pronounced at lower densities. As seen from Fig. 3 for $r_s = 3$ the total transresistivity beyond the RPA as a function of temperature shows no peak at all and this is in stark contrast to the peaked behavior of the transresistivity within the RPA. The disappearance of the large high-temperature plasmon peak results from the strong increase of the drag transresistivity at low temperatures: we ascribe this to the fact that the contribution to drag, made by large-angle inter-layer scattering processes, becomes dominant when the many-body xc corrections are included. The large-angle scattering component strongly enhances the drag for two reasons. First, at low T the e-e scattering phase-space diverges near $x \equiv q/2k_F = 1$. On the other hand, when $x \simeq 1$, the static intra-layer LFF $G_{11}(x)$ becomes close to unity, leading to a reduction of the effective intra-layer interaction $V_{xc,11}(x)$. This by itself weakens the dynamic screening and enhances the drag. Thus, on the background of the large transresistivity at small T, the plasmon-mediated contribution to drag does not result in a peaked behavior of the scaled transresistivity and the total drag rate decreases monotonically in T.

Lack of experimental measurements of the drag at high temperatures does not allow for the time being an experimental verification of our predictions on the position and strength of the plasmon peak in low density bilayers. Notice however that the low temperature peak of the transresistivity and its monotonous behavior at high temperatures, observed in the experiment on hole samples in Ref. [2], by implication support our prediction. At low temperatures, as shown in Fig. 4, our numerical results are in reasonably good agreement with the experimental findings by Kellogg *et al.* [3]. It is clear that the introduction of the effective e-e interaction, mediated by the exchange of virtual PO-phonons, reduces noticeably the total drag and results in a better agreement with experiment.

We thank Zhixin Qian for discussions and kindly making the results of his calculations accessible prior to publication. We acknowledge support from the Korea Science and Engineering Foundation Grant No. R05-2003-000-11432-0 and NSF Grant No. DMR-0313681.

References

[1] *Quantum Theory of the Electron Liquid*, G. F. Giuliani and G. Vignale, (Cambridge University Press, Cambridge, 2005), Chapter 10.

[2] R. Pillarisetty *et al.*, Phys. Rev. Lett. **89**, 016805 (2002); Phys. Rev. B **71**, 115307 (2005).

[3] M. Kellogg *et al.*, Solid State Commun. **123**, 515 (2002).

[4] A.-P. Jauho and H. Smith, Phys. Rev. B **47**, 4420 (1993).

[5] N. P. R. Hill *et al.*, Phys. Rev. Lett. **78**, 2204 (1997).

[6] H. Noh *et al.*, Phys. Rev. B **58**, 12 621 (1998).

[7] K. Flensberg and Ben Yu-Kuang Hu, Phys. Rev. Lett. **73**, 3572 (1994); Phys. Rev. B **52**, 14796 (1995).

[8] L. Świerkowski, J. Szymański, and Z. Gortel, Phys. Rev. Lett. **74**, 3245 (1995); Phys. Rev. B **55**, 2280 (1997).

[9] E. H. Hwang *et al.*, Phys. Rev. Lett. **90**, 086801 (2003).

[10] A. Yurtsever, V. Moldeveanu, and B. Tanatar, Solid State Commun. **125**, 575 (2003).

[11] A. Rojo, J. Phys.: Condens. Matter **11**, R31 (1999).

[12] L. Zheng and A. H. MacDonald, Phys. Rev. B **48**, 8203 (1993)

[13] B. Y.-K. Hu, Phys. Rev. B **57**, 12345 (1998).

[14] S. Adachi, J. Appl. Phys. **58**, R1 (1985).

[15] Z. Qian and G. Vignale, Phys. Rev. B **65**, 235121 (2002); Z. Qian, preprint.

[16] B. Davoudi *et al.*, Phys. Rev. B **64**, 153101 (2001); *ibid* **64**, 233110 (2001).